Thermal imaging through ordered bundles of infrared-transmitting silver-halide fibers

E. Rave, D. Shemesh, and A. Katzir

Citation: Applied Physics Letters **76**, 1795 (2000); doi: 10.1063/1.126168
View online: http://dx.doi.org/10.1063/1.126168
View Table of Contents: http://scitation.aip.org/content/aip/journal/apl/76/14?ver=pdfcov
Published by the AIP Publishing

Thermal imaging through ordered bundles of infrared-transmitting silver-halide fibers

E. Rave,[a] D. Shemesh, and A. Katzir
Raymond and Beverly Sackler Faculty of Exact Science, School of Physics and Astronomy, Tel-Aviv University, Tel-Aviv, Israel 69978

(Received 5 August 1999; accepted for publication 7 February 2000)

Ordered bundles of infrared-transmitting silver-halide ($AgCl_xBr_{1-x}$) fibers were fabricated by extrusion. Bundles of total area 5–20 mm^2 and lengths 5–50 cm included 100–2500 individual fibers and the packing fraction was 0.2–0.3. Each of the individual fibers was transparent in the spectral range 3–30 μm, and therefore, the whole bundle was suitable for thermal imaging. The modulation transfer function was studied using the ''bar chart'' and the ''knife-edge'' methods. The resolution was found to be 4–5 lines/mm for a 900 fiber bundle. Thermal images of objects at room temperature were transmitted from the entrance ends to the exit ends of the bundles. © *2000 American Institute of Physics.* [S0003-6951(00)02014-3]

Ordered (''coherent'') bundles of glass fibers have been widely used for imaging in the visible and they have been the main building blocks of fiberoptic endoscopes.[1] Imaging through such a flexible bundle is normally carried out using a small charge-coupled-device (CCD) camera that is attached to the proximal end of the bundle. There has been an interest in extending this concept to the middle-infrared spectral range 3–30 μm for fiberoptic thermal imaging. The idea is to replace the silica-based glasses, which are totally opaque in the mid-IR, by infrared transmitting fibers, and the standard CCD, by a thermal camera. Such a system will make it possible to carry out thermal imaging in areas that are not easily accessible, such as inside enclosed spaces or inside the human body. Several papers discussed the use of flexible bundles of infrared-transmitting chalcogenide glass fibers[2–5] for thermal imaging. However, most of these glasses do not transmit well above 8 μm and they are not useful for thermal imaging of bodies at room temperature. In the past, we reported preliminary results[6] obtained with bundles of fibers made of crystalline sliver halides. In this work, we discuss the development of improved fiber bundles and their optical characterization.

Single crystals of silver halides of composition $AgCl_xBr_{1-x}$ $(0 \leqslant x \leqslant 1)$ have wide transparency windows in the mid-IR. The mechanical and optical properties[7] of the crystals vary with composition, and in particular, the refractive index at $\lambda = 10.6$ μm increases from 1.98 (pure AgCl) to 2.16 (pure AgBr). Unclad optical fibers have been prepared in our laboratory by extruding single crystals of $AgCl_xBr_{1-x}$ through small dies. These fibers are flexible, nontoxic, and nonhygroscopic, and their transmission losses are of the order of 0.2 dB/m at $\lambda = 10.6$ μm. Unclad fibers have been used for delivering CO_2 laser power, for noncontact thermometry, and for infrared spectroscopy.[8] One may also prepare a compound preform, consisting of a rod of $AgCl_xBr_{1-x}$ inside a tube of composition $AgCl_yBr_{1-y}$ with $y > x$ (i.e., lower index of refraction). Core-clad fibers were fabricated by extruding such a ''rod in tube'' preform through a die. The core-clad fibers made in our group had smaller numerical aperture than the unclad fibers, but the optical losses were higher.

We have fabricated ordered bundles[9,10] of fibers using extrusion methods. In the first step, a length of several meters of clad fiber was extruded through a die. In the second step, this length was cut to many short segments, and all these segments were ordered side by side. The ordered array of segments was inserted into a tube made of pure AgCl. The tube with the ordered segments was used as a new preform, which was extruded through a die. The result was an ordered bundle of 10–100 individual fibers (i.e., multifiber). In the third step, the ordered bundle was cut to short segments, and these segments were ordered in an array and placed in a AgCl tube, which served as a new preform which was extruded through a die. Using this multiple extrusion method, we incorporated 100–2500 fibers in bundles of areas 5–20 mm^2 and lengths 5–50 cm. The thinner bundles were flexible. The core diameters of the individual fibers were between 50 and 250 μm. In former attempts to characterize the imaging properties of our bundles, a blackbody infrared source irradiated the distal end of a bundle, and the proximal end was imaged, using a thermal camera. In those experiments, we observed that the order of the individual fibers in the bundle did not change significantly between the two ends. This has allowed the transmission of thermal images through the bundles. In this work, we characterized the optical properties of some of the improved bundles.

The attenuation of radiation through the bundles was measured using the expression

$$P_{\text{out}} = P_{\text{in}}(1-R)^2 \eta \exp(-\alpha_T L). \tag{1}$$

P_{in} and P_{out} are the average irradiance levels at the input and the output faces of the bundle, respectively, and R is the Fresnel reflection coefficient. L is the bundle length, α_T is the total attenuation coefficient, and η is the fill factor of the bundle, which was 0.26 for all our bundles. To measure the ratio $P_{\text{out}}/P_{\text{in}}$, we used a blackbody source, operating at 60 °C as a target, and measured its power, with and without the fiber bundle. We obtained the attenuation coefficients $\alpha_T = 6.6$ dB/m for the 100 fiber bundles, and $\alpha_T = 13.7$dB/m for the 900 fiber bundles. It is clear that each extrusion step increases the attenuation of the individual fibers.

[a]Electronic mail: eranr@post.tau.ac.il

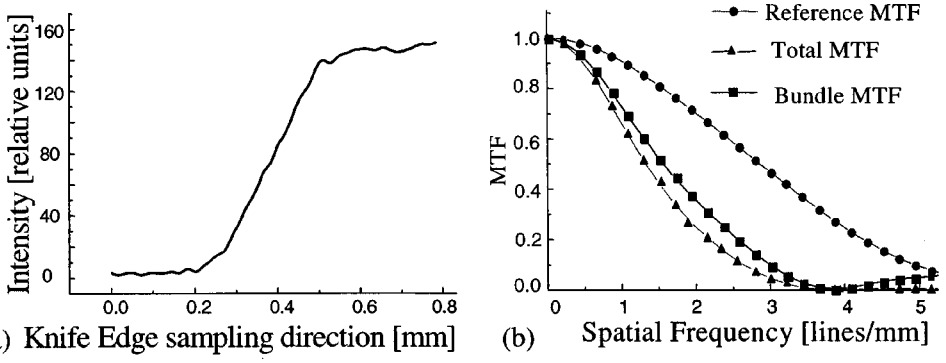

FIG. 1. (a)Knife-edge response of the bundle. (b) MTF of the bundle, obtained by dividing the total MTF by the reference (system) MTF.

In the experiments mentioned below we used a bundle of length 5 cm, and cross-sectional area of 15 mm^2, which consisted of 900 individual elements. The core diameter of each individual fiber was 80 μm.

The modulation transfer function (MTF) (Ref. 11) is defined as the ratio between the modulation M_O of the output signal of the system to the modulation M_I at the input, as a function of the spatial frequency. In principle, one may use at the input of an optical system a sinusoidal signal, whose modulation is $M_I=1$. In practice, it is difficult to fabricate targets with sinusoidal distribution of IR emission, and therefore, we used two other techniques to determine the MTF of the bundles.

One method of measuring the MTF of thermal imaging systems is the process of knife-edge[12] sampling. In our case, a sharp knife edge was kept at $T=60\,^{\circ}\mathrm{C}$, and its image was formed by a lens on the distal end of the bundle. The recorded image (taken at the end proximal) was scanned in a direction perpendicular to the knife edge. We made some standard algebraic operations on this image, which yielded the MTF of the bundle. These include the differentiation of the signal, taking a Fourier transform, and normalizing its magnitude to unity at zero frequency.

Figure 1 shows the results of (a) the knife-edge sampling taken from the fiber bundle, and (b) the MTF that was derived from it. To obtain the bundle MTF, we had to correct for the resolution loss due to the optics, so we took out the bundle and measured the ''reference'' MTF of the optical system. This included the lenses, the IR camera, and the frame grabber electronics. Dividing the total MTF (including the bundle) by the reference MTF, we found the bundle MTF (see Fig. 1). The resolution limit of the bundle was found to be roughly four lines per millimeter.

The second technique for determining the MTF is based on bar targets (spatial square waves). We used several bars to measure the MTF. Each bar was composed of a few black lines of emissivity $\epsilon\approx 1$ that were painted on a metal plate. The width w of each line was equal to the separation d between the lines. We used $w=d$ values between 0.4 and 2.0 mm. We warmed the bar targets to temperatures between 60 and 120 °C. The system response to a bar pattern (square wave) is the contrast transfer function (CTF), and Coltman[13] calculated the relation between the CTF and the MTF:

$$\mathrm{MTF}(f)=\frac{\pi}{4}\left[\mathrm{CTF}(f)+\frac{\mathrm{CTF}(3f)}{3}-\frac{\mathrm{CTF}(5f)}{5}+\frac{\mathrm{CTF}(7f)}{7}-\cdots\frac{\mathrm{CTF}(nf)}{n}\right]. \tag{2}$$

In this case, f is the spatial frequency of the bar target, and nf are its harmonics. An example of the response of our system to a bar target object is shown in Fig. 2. We used a bar with three lines, and a linewidth of $w=d=0.8$ mm. The bar target was heated to 60 °C in Fig. 2(a), and to 120 °C in Fig. 2(b). The target was imaged by the thermal camera through the bundle, and one of the horizontal lines is shown in Fig. 2.

As shown in Figs. 1(a) and 2(a), the primary factor that caused difficulties in the data processing was the noise. The most common source of noise is the counting statistics in the IR detector, due to a small number of incident photons. Noisy images may also occur due to instability in the IR radiation source, that is, the bar target. Instabilities in the detector response, during the time required to scan one image (0.64 s) also contribute to the noise. It is not feasible to compute the contrast of the signal in the figures [1(a) or 2(a)] accurately, because a single pixel exhibiting an extreme intensity value can change the contrast value of the sampled signal. This is bound to cause nonrepeatable and less-reliable MTF results.

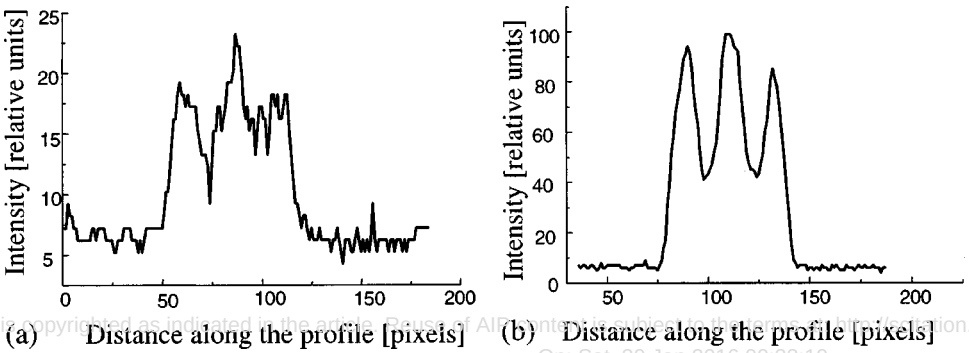

FIG. 2. Intensity profile of a line scanned perpendicular to the orientation of the bars. A bar, which consisted of three lines of linewidth 0.8 mm, was heated to (a) 60 °C and (b) 120 °C.

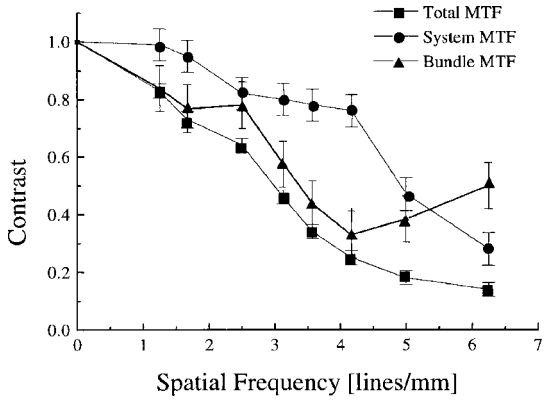

FIG. 3. MTF of the 900 fiber bundle, obtained by dividing the total MTF by the system MTF and by the digital filter MTF.

To improve the signal-to-noise ratio, we applied several digital filters[14] on the line-profile signals. It is clear that the contribution of the noise is dominant at high frequencies, compared to the signal frequency. We used standard average filters (e.g., mean, Gaussian, etc.) that act as low-pass filters. To obtain the bundle MTF we had to correct for the resolution loss due to the optical components, the frame grabber electronics, and the filter MTF. We used Eq. (3) and found the bundle MTF (Fig. 3):

$$\mathrm{MTF}_{\mathrm{bundle}}=\frac{\mathrm{MTF}_{\mathrm{total}}}{\mathrm{MTF}_{\mathrm{system}}\mathrm{MTF}_{\mathrm{filter}}}. \tag{3}$$

These are attempts to measure the resolution of the bundle and we can see that there is still a significant error. The exact resolution limit of the bundle cannot be exactly deduced from these curves. We can only say that the resolution limit of these bundles is better than 5 lines/mm. This value is comparable to the theoretical limit of $R\approx 10$ lines/mm for the bundle, which can be roughly estimated[15] using the formula $R\approx 1/d$, where d is the fiber diameter in mm. We attribute the resolution losses to two factors: (1) the cross talk between adjacent fibers, which is probably caused by the excessive scattering from the core-clad interface; and (2) the infrared light delivered by the cladding material.

The optical setup for thermal imaging was based on a thermal camera (Inframetrics model 600L), operating in the wavelength range of 8–14 μm. The camera contained a nitrogen-cooled HgCdTe single detector and electromechanical scanners. Images of various objects were formed by a lens on the distal end of the bundles, and transmitted through the bundles. Then, they were focused from the proximal end on the detector plane by a germanium lens ($f/4$). The signals obtained from the ''video out'' of the camera were recorded using a PC, and displayed on a TV screen, after digitizing by an 8 bit (256 gray levels) frame grabber. As the operation of frame averaging reduces the random noise, 16 frames were averaged to form a single image file. One example of the image transmitted by the 900 fibers bundle is shown in Fig. 4(b). The object was a tungsten wire heated to 40 °C, (heart shape). The thermal image of the heated object, directly obtained (without the bundle) is shown in Fig. 4(a).

FIG. 4. Thermal image of a tungsten wire (heart shaped) heated to 40 °C, transmitted through the 900 fibers bundle. The scale of the full photograph is 4×4 mm.

In this work, we reported the fabrication of ordered bundles of IR-transmitting silver-halide fibers, using multiple extrusion methods. The optical transmission loss of the bundles is still significantly higher than that of a single fiber. We attribute these losses mainly to excessive scattering from the core-clad interface and to cross talk between adjacent fibers. We determined the MTF of a bundle of 900 fibers, using the bar target and the knife-edge methods. We found that the maximum spatial frequency that could be resolved by the bundle was roughly five lines per millimeter. Thermal images of objects at temperatures 30–70 °C were successfully transmitted through the bundles.

We have recently succeeded in fabricating long and flexible bundles of fibers (e.g., 60-cm-long bundle of diameter 2 mm including 1000 fibers) and are testing them now. In the future, we will fabricate flexible bundle that consist of more than 10 000 individual fibers. We will reduce the transmission losses of the individual fibers in these bundles. With such ordered bundles it would be possible to obtain improved thermal imaging of bodies near room temperature. Fiberoptic thermal imaging will open up new possibilities in science, industry, and medicine.

The authors wish to thank Dr. Adi Arie, Faculty of Engineering, Tel-Aviv University, for helpful discussions.

[1] A. Katzir, *Laser and Optical Fibers in Medicine* (Academic, San Diego, CA, 1993).
[2] M. Saito, M. Takizawa, S. Sakuragi, and F. Tanei, Appl. Opt. **24**, 2304 (1985).
[3] P. Clocek, M. Roth, and R. D. Rock, Opt. Eng. (Bellingham) **26**, 88 (1987).
[4] J. Nishii, T. Yamashita, and T. Yamagishi, Appl. Phys. Lett. **59**, 2639 (1991).
[5] R. Hilton, Sr., R. Hilton, Jr., J. McCord, G. Whaley, T. J. Lorentz, and P. Modlin, Proc. SPIE **3596**, 64 (1999).
[6] D. Shemesh, I. Paiss, S. Shalem, and A. Katzir, Proc. SPIE **2396**, 95 (1995).
[7] A. German and A. Katzir, J. Mater. Sci. **31**, 5109 (1996).
[8] F. Moser, D. Bunimovich, A. DeRow, O. Eyal, A. German, Y. Gostal, A. Levite, N. Barkay, A. Ravid, V. Scharf, S. Shalem, D. Shemesh, R. Simchi, I. Vasserman, and A. Katzir, IEEE J. Quantum Electron. **2**, 872 (1996).
[9] I. Paiss and A. Katzir, Appl. Phys. Lett. **61**, 1384 (1992).
[10] I. Paiss, F. Moser, and A. Katzir, Fiber Integr. Opt. **10**, 275 (1991).
[11] J. W. Goodman, *Introduction to Fourier Optics*, 2nd printing (McGraw-Hill, New York, 1998).
[12] P. Alexis and M. Jonatan, Opt. Eng. (Bellingham) **34**, 1808 (1995).
[13] J. W. Coltman, J. Opt. Soc. Am. **44**, 468 (1954).
[14] Understanding Digital Signal Processing, edited by R. G. Lyons, 2nd printing (Addison-Wesley, Harlow, 1997).
[15] W. G. Driscoll, *Handbook of Optics* (McGraw-Hill, New York, 1978).